



Impact of surface interactions on the phase behavior of Y-shaped molecules



D.P. Ruth^a, R. Toral^b, D. Holz^c, J.M. Rickman^{a,d,*}, J.D. Gunton^a

^a Department of Physics, Lewis Laboratory, Lehigh University, Bethlehem, PA 18015, United States

^b IFISC, (Instituto de Física Interdisciplinar y Sistemas Complejos, CSIC-UIB), Palma de Mallorca, Spain

^c Department of Physics, Hall of Sciences, Drew University, Madison, NJ 07940, United States

^d Department of Materials Science and Engineering, Whitaker Laboratory, Lehigh University, Bethlehem, PA 18015, United States

ARTICLE INFO

Article history:

Received 24 July 2015

Received in revised form 13 November 2015

Accepted 18 November 2015

Available online 23 November 2015

Keywords:

Substrate

Phase transition

ABSTRACT

In recent years the statistical mechanics of non-spherical molecules, such as polypeptide chains and protein molecules, has garnered considerable attention as the phase behavior of these systems has important scientific and health implications. More recently, it has been realized that surface binding may have a considerable impact on this behavior. With this in mind, we examine here the role of surface interactions on the phase behavior of Y-shaped molecules (a simplified model of immunoglobulin) using grand-canonical Monte Carlo simulation. In particular, we investigate the critical behavior of a system of such molecules on a hexagonal lattice using histogram reweighting, multicanonical sampling, and finite-size scaling. After obtaining the critical properties of the three-dimensional bulk system, we investigate the impact of a patterned solid surface on these properties as a function of patterning geometry and surface interaction strength. Our results suggest avenues for tailoring phase behavior by selectively controlling surface characteristics.

© 2015 Elsevier B.V. All rights reserved.

1. Introduction

Molecules adsorbed on thin solid surfaces often self-organize into highly-ordered states and, in recent years, there has been growing interest in the phase behavior of adsorbed molecules having unusual architectures. One important example of this phenomenon is the self-assembly of Y-shaped immunoglobulin (IgG) molecules, which are multidomain proteins that bind to antigens with remarkable specificity. Such antibodies are of substantial relevance in the pharmaceutical world due to their efficacy as therapeutic molecules, as evidenced by the large number that are either approved or in clinical trials for treating human disorders (e.g., cancer, rheumatoid arthritis, osteoporosis, and asthma) [1–3]. Beyond immunoglobulin, there is also interest in the novel structures formed by C₃-symmetric, Y-shaped organic functional molecules (tripods). In this regard, Szabelski et al. [4] have studied a model of tripods on a graphite surface, as described by a two-dimensional, hexagonal lattice, using parallel tempering Monte Carlo simulation. They examined the effect of molecular size on the stability of phases having different morphologies while, for simplicity, ignoring surface interactions.

Surface interactions are, however, an important factor in determining the phase behavior of adsorbed molecules, and various simulational and experimental studies have highlighted the role of these interactions

in determining phase stability. For example, Rzyzsko and Borowko simulated systems of both homonuclear [5] and heteronuclear [6] dimers adsorbed on heterogeneous surfaces and found that the associated phase behavior of the resulting films was strongly affected by the spatial distribution and strength of surface binding sites. In related work, the same authors [7] examined the adsorption of trimers having different configurations on a square lattice and found that trimer chemistry and shape can substantially alter the topology of the associated phase diagram. On the experimental front, the controlled adsorption of macromolecules, such as proteins, can be exploited to develop new biomedical applications and, in some cases, to promote cell adhesion [8]. More specifically, in the case of IgG, studies have indicated that surface adsorption of IgG may be related to the modulation of adherent macrophage behavior [9]. (However, in these studies the Y molecules are not aligned only in the plane, but have some alignment perpendicular to the plane, in contrast to our model presented below.) Indeed, the importance of IgG adsorption has motivated the development of models that reflect IgG/surface interactions to describe observed kinetic behavior [10].

In this work we assess the role of surface interactions on the phase behavior of a simplified model of a Y-shaped molecule, as reflected in the critical temperature, for a system having a particular surface interaction strength parameter, ϵ , and surface geometry. In particular, we calculate the critical temperature, T_c , for a given system by employing grand-canonical Monte Carlo (GCMC) simulations in conjunction with histogram reweighting and multicanonical biasing methods. For concreteness, we consider a patterned surface comprising alternating

* Corresponding author at: Department of Physics, Lewis Laboratory, Lehigh University, Bethlehem, PA 18015, United States.

interacting/noninteracting strips of width, w . After examining the dependence of T_c on ε and w , we suggest possible strategies for tailoring phase behavior via surface patterning.

For simplicity, we employ here a two-dimensional model of the adsorbed, Y-shaped molecule based on the results of some recent studies. For example, Zhao et al. [11] examined the interfacial assembly of Y-shaped antibodies on a silica surface using neutron reflectivity measurements to determine the adsorption geometry of the molecules. They found that these molecules adsorbed predominantly in a “flat on” configuration. In a completely different system, Godlewski et al. [12] studied the physisorption of aromatic Y-shaped molecules on a Ge (001) surface to characterize the electronic structure of adsorbed molecules that are the basis for single-molecule logic circuits. They found that a flat aromatic molecule interacts strongly with dangling bonds on this surface without any significant alteration of its planar structure. Thus, the use of an approximate two-dimensional model of adsorption is an appropriate, simplified description of Y-shaped molecular adsorption in this context.

2. Model and simulation

Our model of a Y-shaped molecule is implemented within the environment of a two-dimensional hexagonal lattice with side length L that contains L^2 sites and is subject to periodic boundary conditions. Each of the N molecules occupies 4 lattice sites, including one central site and sites associated with 3 rigid, *distal* arms. With this geometry, the maximum number density of the system ρ is, therefore, 0.25. In this study, the interactions are those between distal arms and their respective

nearest-neighbor distal arms, each with interaction strength J , as shown in Fig. 1a. For simplicity, there are no center-to-center or center-to-distal arm interactions. In addition, there is a patterned surface comprising alternating interacting/noninteracting strips, each having a width w . Each surface site covered by a Y-molecule is associated with a binding energy, ε . Thus, the total energy of the system is the summation of all distal arm–distal arm interactions and surface interactions. As is customary, all quantities are expressed in units of J .

We performed GCMC simulations to obtain equilibrium configurations for this model system. To analyze the resulting data and obtain the associated critical behavior, we use the Bruce–Wilding finite-size scaling (FSS) techniques [13], [14], along with histogram reweighting and multicanonical sampling methods [15]. The fact that the order parameter for this model (defined below) is a scalar suggests that this Y-molecule model belongs to the Ising universality class, as we demonstrate below.

Assuming that our model belongs to the Ising universality class, the critical point of our system can be determined by matching the probability density function (PDF) of the ordering operator M of our system with the universal distribution of the two-dimensional Ising class. The order parameter M for the fluid is given by [13], [14].

$$M = \frac{1}{1-sr} [\rho - su], \quad (1)$$

$u = U/N$ is the energy density, and s and r are system specific parameters to be determined later. Similar to the order parameter M , the energy-like parameter ε is given by

$$\varepsilon = \frac{1}{1-sr} [u - r\rho]. \quad (2)$$

The Ising universality class has two relevant scaling fields, namely h , the ordering scaling field, and τ , the thermal scaling field. For fluids in this universality class, τ and h are defined as

$$\tau = \omega_c - \omega + s(\mu - \mu_c), \quad h = \mu - \mu_c + r(\omega_c - \omega), \quad (3)$$

where $\omega = J/kT$, μ is the reduced chemical potential in units of kT , and the subscript c denotes the critical point. The parameters r and s determine the degree of mixing in the relative scaling fields, as well as M and ε .

During a simulation of a system size having side L , at fixed values of the rescaled chemical potential μ and inverse temperature ω , we record the molecule number density ρ and the energy density u , from which we determine the joint probability density function $P(\rho, u)$. The joint PDF, $P(M, \varepsilon)$, for the rescaled variables M and ε is related to the joint distribution of density and energy such that $P(M, \varepsilon) = (1-sr)P(\rho, u)$. We focus mostly on the order parameter PDF, namely the marginal density $P(M) = \int d\varepsilon P(M, \varepsilon)$. At the critical point, all members of the Ising universality class have the same fixed point distribution function $\tilde{P}(M)$. Typically, this fixed point distribution is expressed as $\tilde{P}_M(x)$, where $x = \alpha_M^{-1} L^{\beta/\nu} (M - M_c)$. $\beta = 1/8$ and $\nu = 1$ are the critical exponents of the order parameter and correlation length of the two-dimensional Ising class, respectively. α_M^{-1} is a scaling parameter such that $\tilde{P}_M(x)$ has unit variance. Therefore, the PDF $P_L(x)$ of our model must also match $\tilde{P}_M(x)$ at the fixed point.

The fixed point function $\tilde{P}_L(x)$ for the two-dimensional Ising model has been determined from previous work [13]. To match the assumed fixed point distribution, one varies the simulation parameters, namely ω and μ , and, in addition, the scaling parameter s so that the numerically obtained $P_M(x)$ coincides with $\tilde{P}_M(x)$. To simplify matters slightly, we obtain the final scaling parameter r from the slope of the μ – ω coexistence line at criticality [14].

Our GCMC simulation procedure can be summarized as follows. We employ histogram reweighting and the Bruce–Wilding FSS techniques

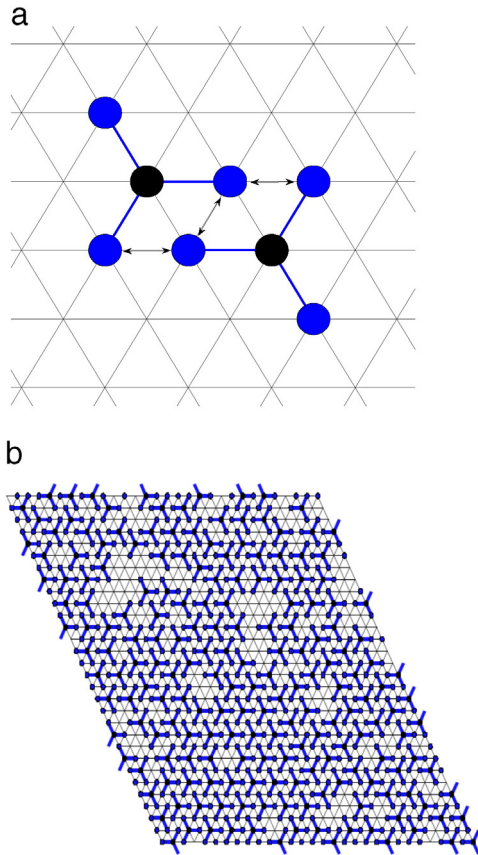


Fig. 1. a.) A schematic of Y-molecules. Each center (black circle) and arm (blue circle) occupy one lattice site, and each arm is physically bonded to the center (solid line). The interactions between arms and their nearest neighbors are denoted by \leftrightarrow . b.) A snapshot of a system containing $L = 30$ molecules and temperature $T = 0.99$ having a corresponding number density $\rho = 0.216$. (For interpretation of the references to color in this figure legend, the reader is referred to the web version of this article.)

[13,14,16,17] to obtain T_c for the infinite system from simulations in which $L = 30, 40, 50,$ and 60 . The observables recorded during the simulation were u and ρ , from which $P(\rho, u)$, $P(\rho)$ and $P(M, \varepsilon)$ were calculated. We employ an ergodic algorithm in which each Monte Carlo step (MCS) comprises N attempts to change the system, either by a molecule translation, rotation, insertion, or removal. Prior to recording u and ρ , the system evolved for 5000–6000 MCS (15,000–25,000 MCS) for those simulations implementing (not implementing) biasing. These quantities are then recorded a total of 150,000–250,000 times over the course of the simulation. A typical configuration for $L = 30$ molecules having a corresponding number density $\rho = 0.216$ is shown in Fig. 1b.

3. Results

We first investigate the phase behavior of the system in the absence of surface interactions. The coexistence curve was determined through a series of GCMC simulations at varying temperatures below the critical region, implementing the histogram reweighting and multicanonical sampling techniques [15] discussed previously. Coexistence between two phases at a temperature T is confirmed when the areas underneath the two peaks in the density distribution $P(\rho)$ are equal. The peak densities are then recorded and plotted on the phase diagram. Examples of several density distributions for varying T at coexistence are shown in Fig. 2a. The corresponding phase diagram, showing the coexistence between low-density and high-density fluid phases, is presented in Fig. 2b. This diagram was constructed from the positions of the peaks in $P(\rho)$ and, as a check, from the average density of each the two phases present. The FSS estimate of T_c is also plotted. Finally, we fit the points of our phase diagram to a power law of the form [16]

$$\rho \pm \rho_c = \alpha |T - T_c| \pm b |T - T_c|^\beta, \quad (4)$$

where β is the two-dimensional Ising model order parameter exponent. This fit is also presented in Fig. 2b. It is worth noting that although there is a small asymmetry evident on the high-density side of the phase diagram, it is not of the type found in the phase diagram of, for example, IgG. This disparity is due, at least in part, to the two-dimensional nature of our model and the fact that we have not taken into account the large excluded volume effect that characterizes IgG [19].

We next obtain the three-dimensional (3D) bulk critical temperature, T_c , for the system in the absence of surface interactions. For this purpose, we first determined that $r = -6.11$ from the slope of the μ - w coexistence line at criticality. Next, we plot $P_L(x)$ for varying system sizes L and determine the best fit to the universal fixed point function $\tilde{P}_M(x)$ by varying $T_c(L)$, $\mu_c(L)$, and s [18]. A sample best fit of $P_L(x)$ to this fixed point function is shown in Fig. 3. As is evident from the figure, within the accuracy of this study, our model belongs to the Ising universality class, as expected.

For completeness, we now describe the extrapolation of our results to the 3-D bulk limit. In particular, we employ the FSS predictions [16] that

$$T_c - T_c(L) \propto L^{-(\theta+1)/\nu} \quad (5)$$

and

$$\mu_c - \mu_c(L) \propto L^{-(\theta+1)/\nu}, \quad (6)$$

to determine the 3-D bulk values of the critical temperature and critical chemical potential. Both the 3-D bulk and the apparent (i.e., L -dependent) critical quantities are obtained by fitting $P_L(x)$ to the fixed universal distribution $\tilde{P}_M(x)$. In Eqs. (5) and (6) θ is a correction to scaling exponent. We use $\theta = 1.35$, as calculated by Barma and Fisher [20], and that coincides with the value conjectured by Nienhuis [21] for the two-dimensional Ising system. To determine 3-D bulk quantities,

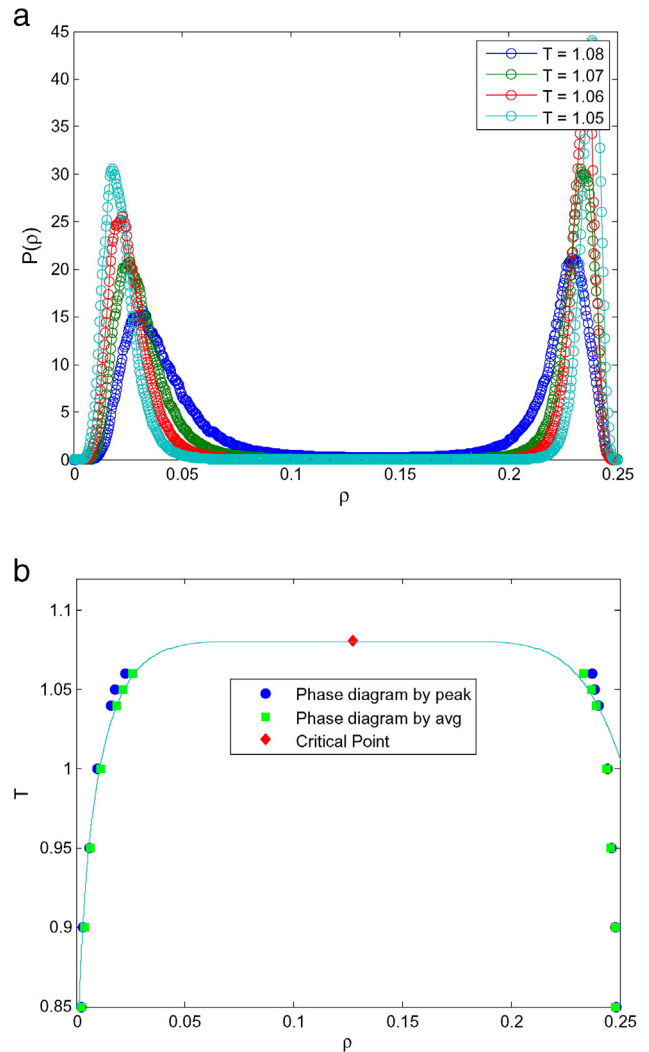


Fig. 2. a.) Plot of estimated $P(\rho)$ versus ρ for varying temperatures at coexistence. All $P(\rho)$ curves were determined as described in the text. b.) The phase diagram obtained from the bimodal PDF $P(\rho)$. This diagram highlights the coexistence of low-density and high-density phases as a function of temperature. The values obtained from the positions of the maxima (circles) of the probability distribution functions and from the average values are plotted (squares) as a function of temperature. Also shown is the best fit to data through T_c and ρ_c of the form $\rho \pm \rho_c = a|T - T_c| \pm b|T - T_c|^\beta$ with $a = 0.05$ and $b = 1.65$.

we plot both $T_c(L)$ and $\mu_c(L)$ versus $L^{-(\theta+1)/\nu}$ and then extrapolate to infinite system size, as shown in Fig. 4a and b. It is found that $T_c = 1.081$ and $\mu_c = -6.659$, respectively.

Having studied the system without a surface, we next consider the impact of a surface on the critical properties of this model. For simplicity, we restrict our attention to finite system sizes. Following the procedure outlined above, we calculated $T_c(L)$ as a function of binding strength ε for $L = 48$ with $w = 2$ for the aforementioned patterned surface, as shown in Fig. 5. As is evident from the figure, $T_c(L)$ decreases by about 15% over the range of interaction strengths considered here, implying that the surface alters the critical behavior of this system. We note that we were unable to obtain $T_c(L)$ for larger values of ε using the procedure outlined above as $P_L(x)$ did not exhibit a double-peaked structure. One might therefore speculate that, for large ε , the nature of the phase transition changes as the energetics of the system is dominated by surface binding.

Finally, we consider the role of surface patterning in determining critical behavior. In particular, $T_c(L)$ was calculated as a function of strip width w for $L = 48$ with $\varepsilon = 0.5$, as shown in Fig. 6. Two comments are in order here. First, the reason that $T_c(L)$ is the same for $w = 0$ and

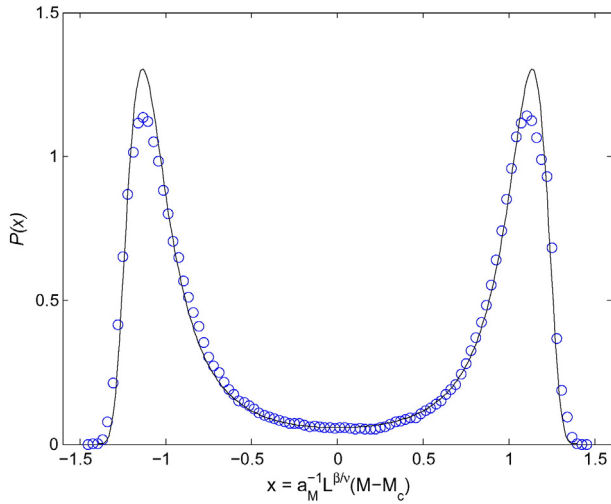


Fig. 3. $P_i(x)$ (blue circle) for $L = 60$ and the universal fixed point distribution $\bar{P}_M(x)$ (line) versus x . a_M^{-1} is a scaling parameter such that $\bar{P}_M(x)$ has unit variance. From this analysis one finds that $T_c(L) = 1.08$ and $\mu_c(L) = -6.48$. (For interpretation of the references to color in this figure legend, the reader is referred to the web version of this article.)

$w = 1$ is that, given the geometry of the Y-molecule, for $w = 1$ the energy of the system is simply shifted by a constant value from that in the absence of a surface (i.e., $w = 0$). Second, the overall decrease in $T_c(L)$ over the range of widths considered here is rather modest (about 3%), suggesting that surface geometry is not as important as interaction strength in determining critical behavior.

4. Conclusions

We employed grand-canonical Monte Carlo (GCMC) simulation to investigate the critical behavior of a system of Y-molecules that are adsorbed on a hexagonal lattice surface having a side length L . After calculating the critical temperature in the absence of surface interactions, we assessed the impact of surface patterning on the critical temperature, $T_c(L)$, as a function of patterning geometry and surface interaction strength. The surface comprises alternating interacting/noninteracting strips, each having a width w , with each surface site having an interaction strength ϵ . It was found that $T_c(L)$ decreases with increasing ϵ and increasing w , indicating that tailoring the surface provides a means for “tuning” the critical properties of the system.

For this model we have demonstrated the coexistence of low- and high-density fluid phases for temperatures below $T_c(L)$. As a practical matter, the manipulation of critical properties may be employed to promote the nucleation of a new phase in a metastable background. In particular, near the critical point, large density fluctuations amplify nucleation kinetics while the lowering of the nucleation barrier also leads to an enhancement of the nucleation rate [22]. Thus, by varying surface interaction strength and geometry, one can effectively manipulate nucleation kinetics.

The results of this work suggest further research directions. As noted by Zhao et al. [11] the interfacial adsorption of proteins is intrinsic to different technological applications and, in particular, the decoration of biomaterial surfaces can be used to improve surface selectivity and biocompatibility. It is therefore useful to consider the impact of various surface patterns on selectivity and adsorbate geometry. With this in mind, it would be useful to consider other surface patterns, such as those comprising a checkerboard or a spatially random distribution of binding sites. The aim here is to determine which patterning characteristics lead to desirable molecular orientations. In addition, one might also explore the regime in which surface interactions are dominant (i.e., large ϵ) to determine whether the nature of the phase transition changes. These possible research avenues are the subject of ongoing work.

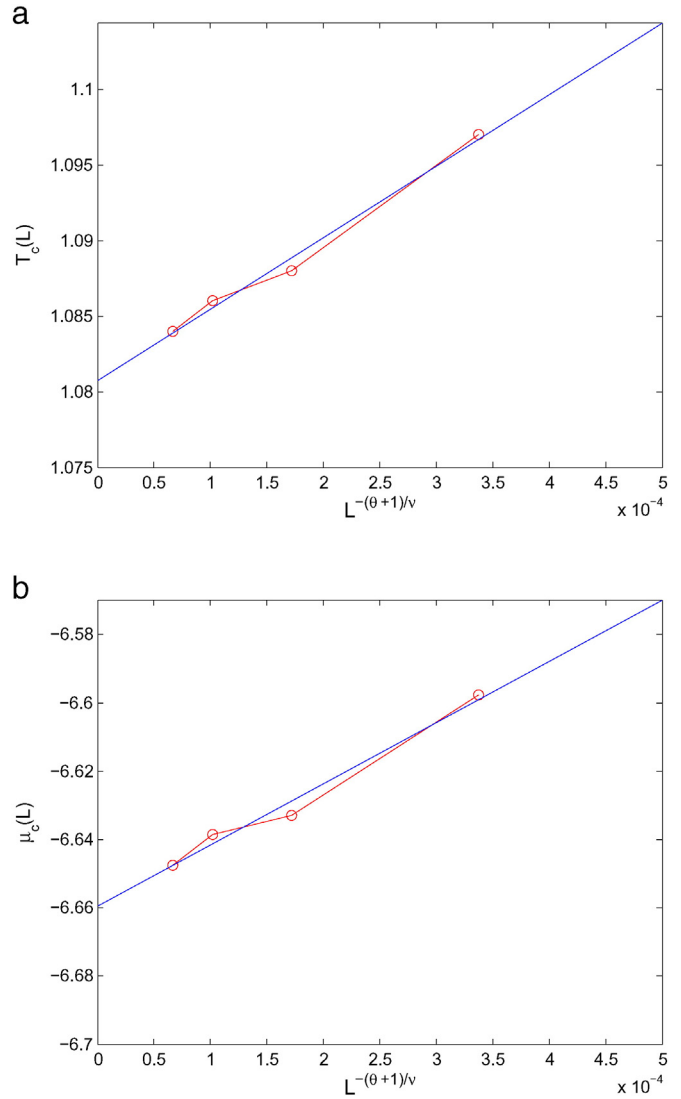


Fig. 4. a.) Plot of the apparent 3-D bulk critical temperature determined from matching $P_i(x)$ to $\bar{P}(x)$. b.) Plot of the apparent 3-D bulk critical chemical potential determined from matching $P_i(x)$ to $\bar{P}(x)$. The extrapolated critical temperature and chemical potential are $T_c = 1.081$ and $\mu_c = -6.659$, respectively.

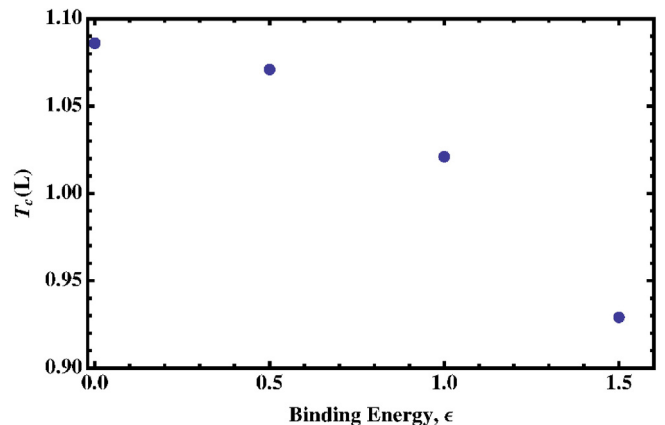


Fig. 5. The critical temperature, $T_c(L)$, versus surface binding strength, ϵ , for a system having $L = 48$ and a strip width $w = 2$.

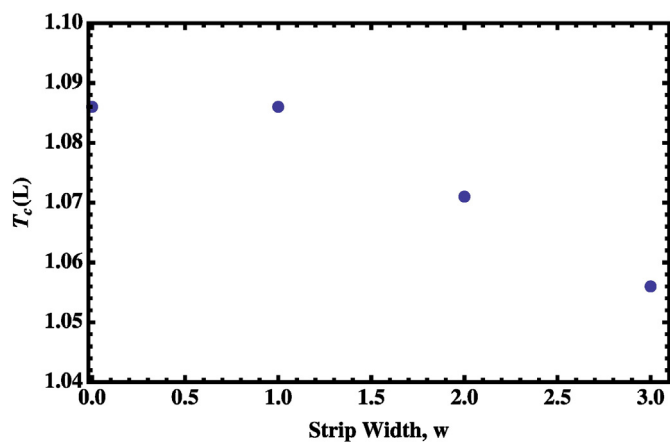


Fig. 6. The critical temperature, $T_c(L)$ versus strip width, w , for a system having $L = 48$ and a patterned surface with $\varepsilon = 0.5$.

Acknowledgements

This work was supported by a grant from the G. Harold and Leila Y. Mathers Foundation (541974). RT acknowledges financial support from EU (FEDER) and the Spanish MINECO under Grant INTENSE@COSYP (FIS2012-30634). DH acknowledges financial support from NSF PHY-0849416 and PHY-1359195.

References

- [1] K. Maggon, Monoclonal antibody "gold rush", *Curr. Pharm. Biotechnol.* 14 (2007) 1978.
- [2] J.M. Reichert, Monoclonal antibodies as innovative therapeutics, *Curr. Pharm. Biotechnol.* 9 (2008) 423.
- [3] J.M. Reichert, C.J. Rosensweig, L.B. Faden, M.C. Dewitz, Monoclonal antibody successes in the clinic, *Nat. Biotechnol.* 23 (2005) 1073.
- [4] P. Szabelski, W. Rzyzko, T. Pancyzk, E. Ghijssens, K. Tahara, Y. Tobe, S. De Feyter, Self-assembly of molecular tripods in two dimensions: structure and thermodynamics from computer simulation, *RSC Adv.* 3 (2013) 25159.
- [5] M. Borowko, W. Rzyzko, Critical behavior of dimers in monolayers adsorbed on heterogeneous solid surfaces, *J. Colloid Interface Sci.* 244 (2001) 1 bf.
- [6] W. Rzyzko, M. Borowko, Monte Carlo study of adsorption of heteronuclear dimers on heterogeneous surfaces, *Thin Solid Films* 425 (2003) 304.
- [7] W. Rzyzko, M. Borowko, Computer simulation of phase diagrams of trimers adsorbed on a square lattice, *Phys. Rev. B* 67 (2003) 045403.
- [8] V. Hlady, J. Buijs, Protein adsorption on solid surfaces, *Curr. Opin. Biotechnol.* 7 (1996) 72–77.
- [9] C.R. Jenney, J.M. Anderson, Adsorbed serum proteins responsible for surface dependent human macrophage behavior, *J. Biomed. Mater. Res.* 49 (2000) 435.
- [10] E.A. Kulik, I.D. Kalinin, V.I. Sevastianov, The heterogeneity of protein/surface interactions and structural alterations of adsorbed albumin and immunoglobulin, *J. Artif. Organs* 15 (1991) 386–391.
- [11] X. Zhao, F. Pan, J.R. Lu, Interfacial assembly of proteins and peptides: recent examples studied by neutron reflection, *J. R. Soc. Interface* 6 (2009) S659–S670.
- [12] S. Godlewski, M. Kolmer, H. Kawai, B. Such, R. Zuzak, M. Saeyns, P. Mendoza, A.M. Echavarren, C. Joachim, M. Szymanski, Contacting a conjugated molecule with a surface dangling bond dimer on a hydrogenated Ge (001) surface allows imaging of the hidden ground electronic state, *ACS Nano* 7 (2013) 10105–10111.
- [13] A.D. Bruce, N.B. Wilding, Scaling fields and universality of the liquid–gas critical point, *Phys. Rev. Lett.* 68 (1992) 193.
- [14] N.B. Wilding, A.D. Bruce, Density fluctuations and field mixing in the critical fluid, *J. Phys. Condens. Matter.* 4 (1992) 3087.
- [15] R. Toral, P. Colet, *Stochastic Numerical Methods*, Wiley-VCH, Weinheim, Germany, 2014.
- [16] N.B. Wilding, Critical-point and coexistence-curve properties of the Lennard–Jones fluid: a finite-size scaling study, *Phys. Rev. E* 52 (1995) 602.
- [17] X. Li, S. Lettieri, N. Wentzel, J.D. Gunton, Phase diagram of a model of nanoparticles in electrolyte solutions, *J. Chem. Phys.* 129 (2008) 164113.
- [18] The use of a parenthetical L (e.g., $T_c(L)$) denotes an apparent quantity associated with a finite system size L .
- [19] Y. Wang, A. Lomakin, R.F. Latypov, J.P. Laubach, T. Hideshima, P.G. Richardson, N.C. Munshi, K.C. Anderson, G.B. Bennedek, Phase transitions in human IgG solutions, *J. Chem. Phys.* 139 (2013) 121904.
- [20] M. Barma, M.E. Fisher, Two-dimensional ising-like systems: corrections to scaling in the Klauder and double-Gaussian models, *Phys. Rev. B* 31 (1985) 5954.
- [21] B. Nienhuis, Analytical calculation of two leading exponents of the dilute Potts model, *J. Phys. A Math. Gen.* 15 (1982) 199.
- [22] J.D. Gunton, A. Shiryayev, D.L. Pagan, *Protein Condensation: Kinetic Pathways to Crystallization and Disease*, Cambridge University Press, Cambridge, UK, 2007.